

R. A. Crawford
University of Tennessee Space Institute

N87-11223

OBJECTIVES

The experimental contract objective is to provide a complete set of "benchmark" quality data for the flow within a "large" rectangular turning duct. These data are to be used to evaluate and verify three-dimensional internal viscous flow models and computational codes. The analytical contract objective is to select such a computational code and define the capabilities of this code to predict the experimental results. Details of the proper code operation will be defined and improvements to the code modeling capabilities will be formulated. Separate but coordinated experimental and analytic approaches are in progress to attain the contract objectives.

APPROACH, EXPERIMENTAL

The experimental facility design features modular tunnel components which allow flow measurements every 15° in the 90° bend. The 25.4 cm (10 in) square cross section tunnel is designed with a 13 to 1 area ratio bell mouth contoured to provide uniform flow velocity and is powered by a variable speed, six-bladed fan. The tunnel is designed for incompressible flow and will produce tunnel velocities of 6 to 20 m/sec (20 to 65 ft/sec). These two flow conditions provide laminar and fully turbulent boundary layer profiles at the entrance to the 90° bend. Corresponding Reynolds numbers based on tunnel width of $Re_d = 98 \times 10^3$ at 6 m/sec and $Re_d = 328 \times 10^3$ at 20 m/sec are significantly higher than the Reynolds number values from NASA-CR-3367 by Taylor, Whitelaw and Yianneskis. Thus the boundary layer thickness in this investigation was also significantly less (1/3) than that reported in NASA-CR-3367. This investigation provides baseline curved duct flow data which is closer to real turbine cascade Reynolds numbers and Dean numbers than previously obtained.

The primary instrumentation is designed for non-intrusive flow measurements utilizing a three-dimensional, laser velocimeter (LV) and wall static pressure gages. The LV utilizes two color beams and Bragg diffraction beam splitting/frequency shifting to separate the three simultaneous, orthogonal, vector velocity components. The LV signal processors determine the digital values of velocity from the seed particles crossing the laser beam probe volume. To improve and speed up digital data acquisition, the LV processors are designed around an S-100 bus Z-80 microprocessor which provides on-line, near-real time data reduction. This on-line data as it is acquired and recorded for off-line detailed analysis. To qualify the measurements as "benchmark" data, the LV data will be compared with both pitot probe and hot wire anemometer measurements for flow conditions which permit comparisons.

RESULTS, EXPERIMENTAL

Following careful checkout and calibration of the experimental facility and instrumentation the curved duct was surveyed with the 3D LV system at six stations (inlet, 0° , 30° , 60° , 90° , exit). Extensive tunnel flow quality surveys were completed in the inlet section following "benchmark" calibration of the LV system, pitot-static, and hot wire anemometer. All three measurement systems were calibrated against reference standards and were found to agree within $\pm 1\%$ on the entrance section velocity. The LV system was calibrated with a spinning disk reference velocity

*NASA Contract NAS3-23278.

at 20 m/sec. The pitot-static pressures were read on a precision slant manometer with 13mm of H₂O full scale. The hot-wire system was calibrated in a reference nozzle flow at 30.5 m/sec. Velocity surveys taken 50.8 cm (20 in) behind the bell mouth exit showed flat velocity profiles \pm 0.5% mean velocity outside of the boundary layer. The mill bed traverse system has demonstrated repeated accuracy of \pm 0.1mm on all three axis movement. Both LV and probe positions are controlled by the computer driven mill bed.

Development and operation of a satisfactory flow seeding system remained a problem during the experimental investigation. Phenolic micro-ballons of equivalent 2-5 micron size were successfully seeded in a water-alcohol slurry and in a fluidized bed air seeder. However the phenolic spheres would become statically charged and collect on screens and tunnel walls. The operational problems of using the micro-ballons were greater than their advantages of small particle lag. Water droplets were selected because of their good scattering characteristics, clean properties and low cost. However water droplet seed must be in the 2-5 micron size range to prevent serious particle lag problems. It is very difficult to control droplet size as temperature, relative humidity and atmospheric dust influence water droplet size. At high tunnel speeds, 20 m/sec, the influence of centrifugal forces caused some particle lag problems in the Y-component velocity measurements.

The experimental investigation is complete with 3-D velocities surveys at six flow stations, 600 spatial points per station, for two bulk flow velocities of 6 m/sec and 20 m/sec. Since each of the 600 point surveys took several days to accomplish, the complete data set was non-dimensionalized on bulk velocity to eliminate small variations in tunnel speed during the testing. Sample results are shown in Figures 1 and 3 for the 60° station. Due to the thinness of the entrance boundary layer the axial and crossflow velocity developments in the turn are driven primarily by the pressure forces.

APPROACH, ANALYTICAL

The analytical approach involves, first, selecting a computer code capable of solving the Navier Stokes equations with turbulence models for three dimensional internal flow, and adapting it to the experimental geometry and flow conditions. After this, calculations are to be made for laminar flow conditions for unheated flow. Analysis of these calculations will define the grid size and stretching factors required for adequate resolution as well as the values of time steps and smoothing factors required for convergence. Also, any output and graphics capability required for comparison with data is to be developed during this phase. The adequacy of the code with respect to the differencing scheme, adaptability and convergence will be decided in this phase, by comparisons with published experimental and computational data and by grid sensitivity studies. After the grid refinement studies to determine grid sensitivity are completed, computations on the curved duct at conditions corresponding to the UTSI experiment will be performed. The analytic results from these computations will be used in detailed comparisons with experimental data.

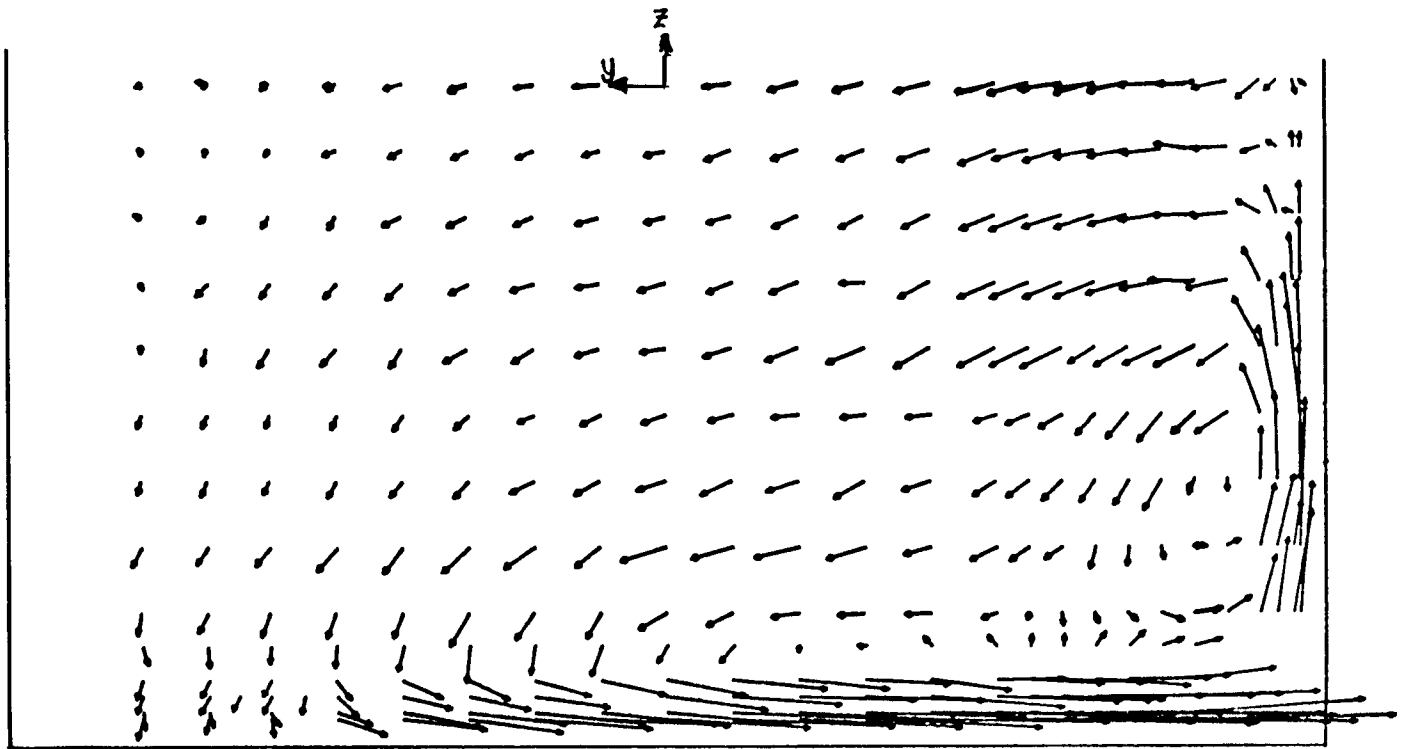
RESULTS, ANALYTICAL

The code selected was based on the Beam-Warming algorithm. It is fully elliptic with all inertial terms retained. Both cross-stream viscous terms are retained, and only the stream-wise viscous term is neglected. The code, developed by P.D. Thomas, uses generalized coordinates and was easily adapted to the curved duct case. Extensive comparisons were made with the analytic results published by Briley and McDonald and with experimental data published by Whitelaw et. al. The comparisons were made for laminar flow to avoid uncertainties due to turbulence modeling. Grid refinement comparisons involving doubling the number of points did not significantly effect the

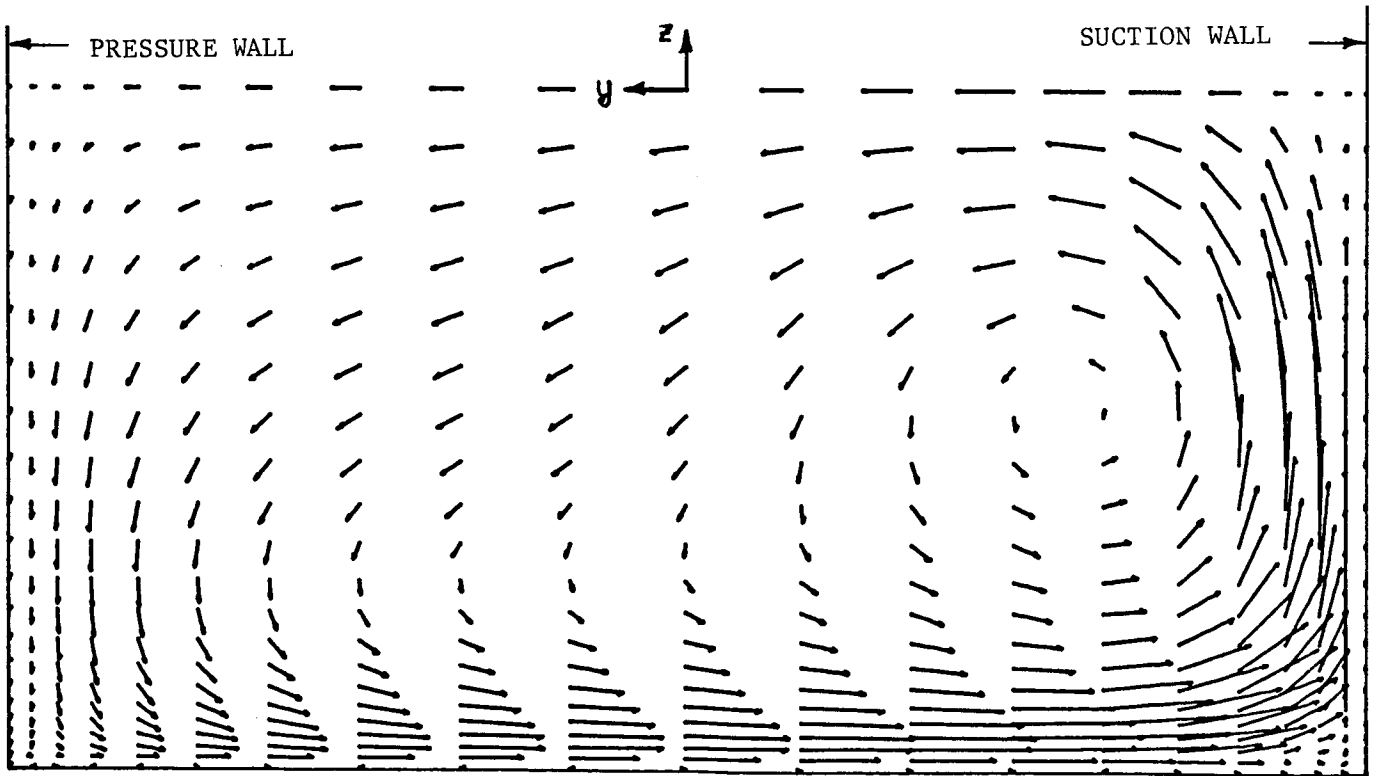
downstream results for the inlet boundary layer profile selected. If a much thinner entrance boundary layer is input the fine grid results may differ from the course grid results.

For the turbulent cases simulating the curved duct experiment, an algebraic eddy viscosity model was used. The sensitivity to initial boundary layer thickness was investigated by comparative runs with 13mm (0.5 in), 25mm (1.0 in) and 51mm (2.0 in) profiles. The 13mm and 25mm solutions were very similar but the 51mm boundary layer was large compared to the tunnel half height and the solution was different. The similarity of the two thin boundary layer solutions especially near the end of the curved duct may indicate an axial numerical diffusion of the boundary layer which would not occur experimentally.

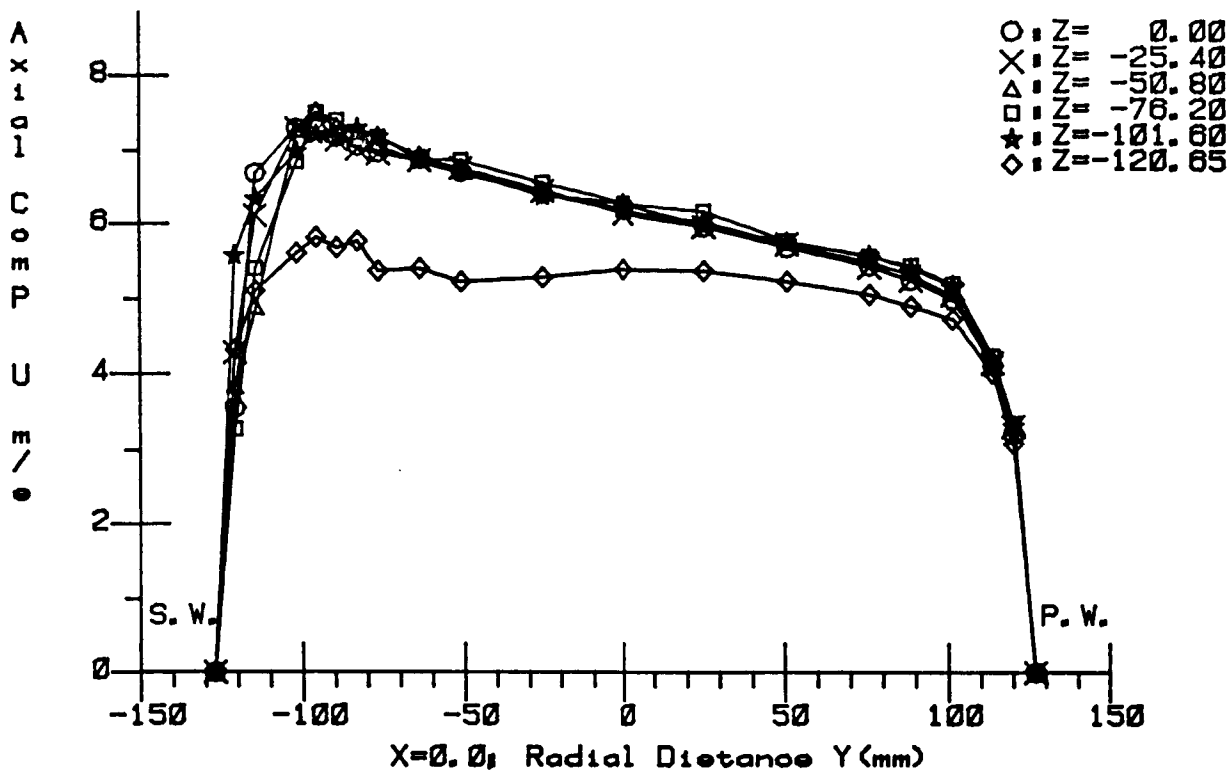
Comparison of the cross-flow and stream-wise velocities at the 60° station from the analytic and experimental cases shows a significant difference. Although the general flow pattern is similar the experimental results show much thinner boundary layers and larger velocity gradients. Figures 1 and 2 compare crossflow velocities at the 60° station. Figures 3 and 4 compare stream-wise velocities at the 60° station. A significant effort remains to complete analysis of all data and explain the differences in theoretical and experimental results.



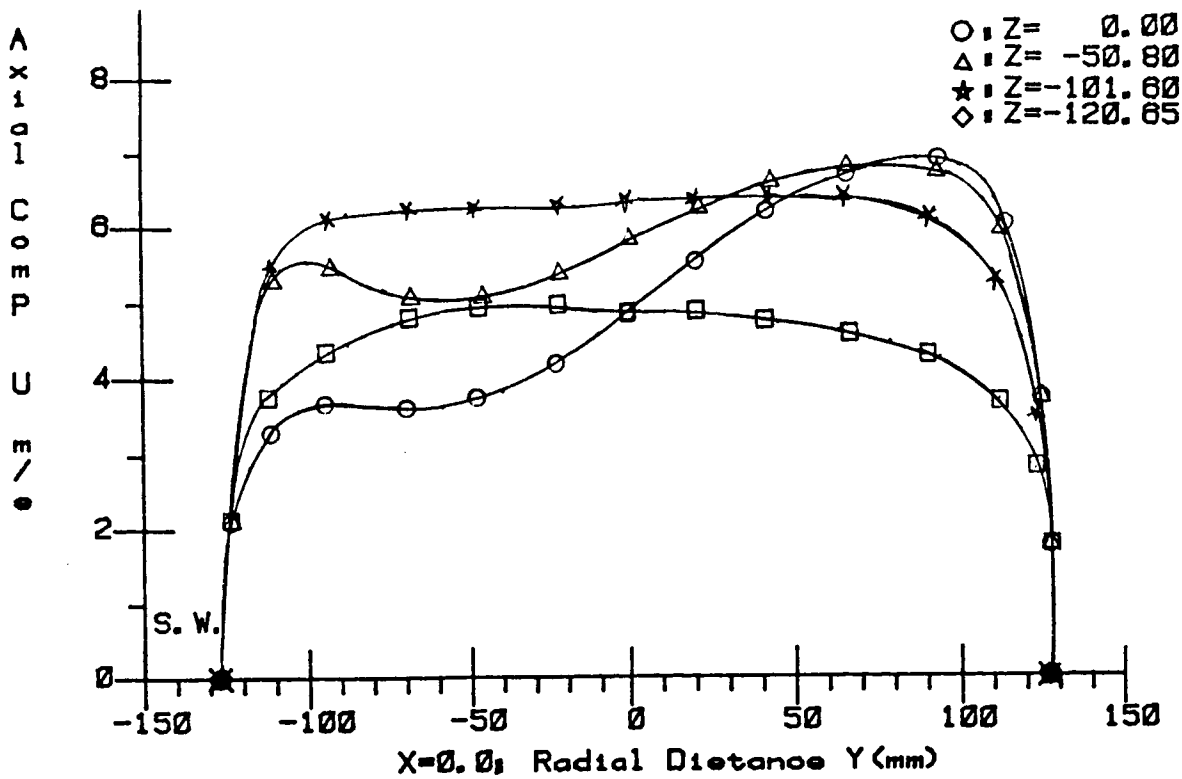
EXPERIMENTAL CROSSFLOW VELOCITY, 60° STATION
 FIGURE 1.



ANALYTIC CROSS FLOW VELOCITY, 60° STATION
 FIGURE 2



EXPERIMENTAL AXIAL VELOCITY, 60° STATION
 FIGURE 3



ANALYTIC AXIAL VELOCITY, 60° STATION
 FIGURE 4